Astrophysical Map Reconstruction from Convolutional Mixtures

K. Kayabol[*,a,1,2], J. L. Sanz[b,1], D. Herranz[b,1], E. E. Kuruoglu[a,1], E. Salerno[a,1]

[a] *ISTI, CNR, via G. Moruzzi 1, 56124, Pisa, Italy*
[b] *IFCA, University of Cantabria, Avda. Los Castros s/n 39005, Santander, Spain*

Abstract

We propose an astrophysical map reconstruction method for multi-channel blurred and noisy observations. We define the problem under Bayesian framework. We use the *t*-distribution to model the image gradients as a prior and resort to Monte Carlo simulation to estimate the maps and the error both in the pixel and frequency domain. We test our method in five different sky patches located at varying positions from galactic plane to high latitude. We give the estimated maps along with the power spectra and the numerical performance measures.

Key words: Bayesian source separation, astrophysical images, student t distribution, Langevin

1. Introduction

The source separation problem in astrophysical images has already been studied in different works [1], [2], [3] and [4]. In this study, we focus on the problem of multi-channel source separation and restoration from multi-channel blurred and noisy observations. We assume that the parameters of the parametric mixing matrix are known or at least estimated with a known error. Under this assumption, we reconstruct the source maps in the pixel domain by using a Monte Carlo technique that has been recently developed and tested on astrophysical source separation problem [4]. Our method is the extended version of the method in [4] to convolutional mixture problem and has also the ability to estimate mixing matrix.

The studies on the separation of convolutional or blurred image mixture can be found in the literature. Castella and Pesquet [5] extended the contrast function based

[*]Corresponding author

Email addresses: koray.kayabol@isti.cnr.it (K. Kayabol), sanz@ifca.unican.es (J. L. Sanz), herranz@ifca.unican.es (D. Herranz), ercan.kuruoglu@isti.cnr.it (E. E. Kuruoglu), emanuele.salerno@isti.cnr.it (E. Salerno)

[1]This work is supported by the Italian Space Agency research program on cosmology and fundamental physics. Partial support from CNR-CSIC bilateral project: "Astrophysical data analysis using nonstationary signal processing techniques".

[2]Koray Kayabol is also supported by the International Center for Theoretical Physics, Trieste, Italy, Training and Research in Italian Laboratories program.

ICA technique in the case of blurring. Anthoine [6] proposed to solve the same problem by adapting the existing variational and statistical methods and modeling the components in wavelet domain. Tonazzini and Gerace [7] use the Markov Random Field (MRF) based image prior in the Bayesian framework. Shwartz et al. [8] address a solution to separation of defocus blurred reflections in the natural scenes by using the sparsity of the Short Time Fourier Transform (STFT) coefficients as priors. In a recent study, multi-channel separation and deconvolution is proposed for document images [9]. We use a Bayesian formulation to include the effects of the antenna apertures and solve the debluring and map reconstruction problems jointly. Since the point spread functions (psf's) of the antennas are known, we easily define our likelihood function by including the psf's.

In the Bayesian framework, we formulate our information on source maps with prior densities. Because of the blurring and the noise, the reconstruction problem is very bad conditioned. This means that we have already lost some detail information on the observed image. The lost information in such a case is found in the high frequency contents of the images. While choosing our image prior, we consider this situation and define a prior such that it models the distribution of the high frequency components of the image. We use the most basic high frequency components of the image, namely the edges of the image. We obtain the edge images by applying a simple horizontal and vertical gradient operator to image. The intensities of the edge images are very sparse and have a heavy-tailed distribution. We exploit the t-distribution as a statistical model for the edge image. The first examples of the use of t-distribution in inverse imaging problems can be found in [10] and [11]. In [11], it is reported that the t-distribution approximates the wavelet coefficients of an image more accurately. In recent papers, it has been used for image restoration [12] and deconvolution [13]. In [4], it is empirically shown that the edge images of the CMB, synchrotron and dust maps are modeled by using t-distribution. This has been used in the Bayesian source separation problem.

We estimate the parameters of the mixing matrix and the parameters of the t-distribution image prior. We give numerical performance measures in the cases where the groundtruths are either known or unknown. We use the MC method to estimate the error.

The organization of the paper is laid out as follows. We introduce the astrophysical component separation problem in the case of convolutional mixtures in Section 2. In Section 3, we define formally the source separation problem in the Bayesian context, and outline the source model, the likelihood and the posteriors. The details of the source maps and parameters estimations are given in Section 4. A number of simulation cases including five different sky patches are given in Section 5, and finally conclusions are drawn in Section 6.

2. Astrophysical Component Separation Problem: Convolutional Mixtures Case

We assume that the observed images, $y_k, k \in \{1, 2, \ldots, K\}$, are linear combinations of L source images. Let the kth observed image be denoted by $y_{k,i}$, where $i \in \{1, 2, \ldots, N\}$ represents the lexicographically ordered pixel index. Taking into account the effect of the telescope and by denoting $\mathbf{s}_l$ and $\mathbf{y}_k$ as $N \times 1$ vector representations of source and observation images, respectively, the observation model can

be written as

$$\mathbf{y}_k = \mathbf{h}_k * \sum_{l=1}^{L} a_{k,l}\mathbf{s}_l + \mathbf{n}_k \tag{1}$$

where the asterisk means convolution, and $\mathbf{h}_k$ is the telescope radiation pattern in the k'th observation channel. The vector $\mathbf{n}_k$ represent an iid zero-mean noise with $\Sigma = \sigma_k^2\mathbf{I}_N$ covariance matrix where $\mathbf{I}_N$ is an identity matrix. Although the noise is not homogeneous in the astrophysical maps, we assume that the noise variance is homogeneous within each sky patch and is also known.

3. Bayesian Formulation of Astrophysical Component Separation

3.1. Source Model

We use the image model previously proposed in [4]. For this purpose, we write an auto-regressive source model using the first order neighbors of the pixel in the direction d:

$$\mathbf{s}_l = \alpha_{l,d}\mathbf{G}_d\mathbf{s}_l + \mathbf{t}_{l,d} \tag{2}$$

where the maximum number of first order neighbors is 8 but we use only 4 neighbors, $d \in \{1, \ldots, 4\}$, in the main vertical and horizontal directions. The matrix $\mathbf{G}_d$ is a linear one-pixel shift operator, α_d is the regression coefficient and the regression error $\mathbf{t}_{l,d}$ is an iid t-distributed zero-mean vector with dof parameter $\beta_{l,d}$ and scale parameters $\delta_{l,d}$. Generally in real images, except the Gaussian distributed ones, the regression error is better modelled by some heavy-tailed distribution. The t-distribution can also model the Gaussian distributed data. Therefore, it is a convenient model for data whose distribution ranges from Cauchy to Gaussian. In [4], the t-distribution has been fitted to simulated CMB, synchrotron and dust maps and gives better results in the sense of mean square error as compared to the Gaussian and the Cauchy densities. The multivariate probability density function of an image modelled by a t-distribution can be defined as

$$p(\mathbf{t}_{l,d}|\alpha_{l,d},\beta_{l,d},\delta_{l,d}) = \frac{\Gamma((N+\beta_{l,d})/2)}{\Gamma(\beta_{l,d}/2)(\pi\beta_{l,d}\delta_{l,d})^{N/2}}\left[1 + \frac{\phi_d(\mathbf{s}_l,\alpha_{l,d})}{\beta_{l,d}\delta_{l,d}}\right]^{-(N+\beta_{l,d})/2} \tag{3}$$

where $\phi_d(\mathbf{s}_l,\alpha_{l,d}) = \|\mathbf{t}_{l,d}\|^2 = \|\mathbf{s}_l - \alpha_{l,d}\mathbf{G}_d\mathbf{s}_l\|^2$ and $\Gamma(.)$ is the Gamma function.

We can write the density of $\mathbf{s}_l$ by using the image differentials in different directions, by assuming the directional independence, as

$$p(\mathbf{s}_l|\alpha_{l,d},\beta_{l,d},\delta_{l,d}) = \prod_{d=1}^{4} p(\mathbf{t}_{l,d}|\alpha_{l,d},\beta_{l,d},\delta_{l,d}). \tag{4}$$

We assume uniform priors for $\alpha_{l,d}$ and $\delta_{l,d}$ and use noninformative Jeffrey's prior for $\beta_{l,d}$; $\beta_{l,d} \sim 1/\beta_{l,d}$.

3.2. Likelihood

Since the observation noise is assumed to be independent and identically distributed zero-mean Gaussian at each pixel, the likelihood is expressed as

$$p(\mathbf{y}_{1:K}|\mathbf{s}_{1:L},\mathbf{A}) \propto \prod_{k=1}^{K} \exp\left\{-\frac{\|(\mathbf{y}_k - \mathbf{H}_k \sum_{l=1}^{L} a_{k,l}\mathbf{s}_l)\|^2}{2\sigma_k^2}\right\} \tag{5}$$

where the mixing matrix $\mathbf{A}$ contains all the mixing coefficients $a_{k,l}$ introduced in (1). We assume uniform prior for $a_{k,l}$. The matrix $\mathbf{H}_k$ is the Toeplitz convolution matrix constituted by $\mathbf{h}_k$ introduced in (1).

3.3. Posteriors

By taking into account the parameters of the source priors, we write the joint posterior density of all unknowns as:

$$p(\mathbf{s}_{1:L},\mathbf{A},\Theta|\mathbf{y}_{1:K}) \propto p(\mathbf{y}_{1:K}|\mathbf{s}_{1:L},\mathbf{A})p(\mathbf{s}_{1:L},\mathbf{A},\Theta) \tag{6}$$

where $\Theta = \{\alpha_{1:L,1:4},\beta_{1:L,1:4},\delta_{1:L,1:4}\}$, $p(\mathbf{y}_{1:K}|\mathbf{s}_{1:L},\mathbf{A})$ is the likelihood and $p(\mathbf{s}_{1:L},\mathbf{A},\Theta)$ is the joint prior density of the unknowns. Here, we also define the mixing matrix as a variable, but in the simulations, we set it to a fixed value. The joint prior can be factorized as $p(\mathbf{s}_{1:L}|\alpha_{1:L,1:4},\beta_{1:L,1:4},\delta_{1:L,1:4})\ p(\mathbf{A})\ p(\beta_{1:L,1:4})\ p(\delta_{1:L,1:4})\ p(\alpha_{1:L,1:4})$. Furthermore, since the sources are assumed to be independent, the joint probability density of the sources is also factorized as

$$p(\mathbf{s}_{1:L}|\Theta) = \prod_{l=1}^{L} p(\mathbf{s}_l|\Theta) \tag{7}$$

For estimating all the unknowns, we write the conditional posteriors of them as

$$\begin{aligned}
p(a_{k,l}|\mathbf{y}_{1:K},\mathbf{s}_{1:L},\mathbf{A}_{-a_{k,l}},\Theta) &\propto p(\mathbf{y}_{1:K}|\mathbf{s}_{1:L},\mathbf{A}) \\
p(\alpha_{l,d}|\mathbf{y}_{1:K},\mathbf{s}_{1:L},\mathbf{A},\Theta_{-\alpha_{l,d}}) &\propto p(\mathbf{t}_{l,d}|\Theta) \\
p(\beta_{l,d}|\mathbf{y}_{1:K},\mathbf{s}_{1:L},\mathbf{A},\Theta_{-\beta_{l,d}}) &\propto p(\mathbf{t}_{l,d}|\Theta)p(\beta_{l,d}) \\
p(\delta_{l,d}|\mathbf{y}_{1:K},\mathbf{s}_{1:L},\mathbf{A},\Theta_{-\delta_{l,d}}) &\propto p(\mathbf{t}_{l,d}|\Theta) \\
p(\mathbf{s}_l|\mathbf{y}_{1:K},\mathbf{s}_{(1:L)-l},\mathbf{A},\Theta) &\propto p(\mathbf{y}_{1:K}|\mathbf{s}_{1:L},\mathbf{A})p(\mathbf{s}_l|\Theta)
\end{aligned} \tag{8}$$

where "–variable" expressions in the subscripts denote the removal of that variable from the variable set.

The ML estimation of the parameters $\alpha_{l,d}$, $\beta_{l,d}$ and $\delta_{l,d}$ using the EM method [16] is given in Section 4.3. To estimate the source images, we use a version of the posterior $p(\mathbf{s}_l|.)$ augmented by auxiliary variables and find the estimation with a Langevin sampler. The details are given in Section 4.

4. Estimation of Astrophysical Maps and Parameters

In this section, we give the estimation of the mixing matrix, source maps and their parameters.

4.1. Mixing Matrix

We assume that the prior of $\mathbf{A}$ is uniform between 0 and ∞. The conditional density of $a_{k,l}$ is expressed as $p(a_{k,l}|\mathbf{y}_{1:K}, \Theta^t_{-a_{k,l}}) \propto p(\mathbf{y}_{1:K}|\Theta^t)$. From (5), it can be seen that the conditional density of $a_{k,l}$ becomes Gaussian. The parameter $a_{k,l}$ is estimated by finding the mode of the posterior analytically.

4.2. Astrophysical Map Estimation

We simulate the astrophysical maps from their posteriors by using MCMC scheme. In the classical MCMC schemes, a random walk process is used to produce the proposal samples. Although random walk is simple, it affects adversely the convergence time. The random walk process only uses the previous sample for producing a new proposal. Instead of random walk, we use the Langevin stochastic equation, which exploits the gradient information of the energy function to produce a new proposal. Since the gradient directs the proposed samples towards the mode, the final sample set will mostly come from around the mode of the posterior. The Langevin equation used in this study is written as

$$\mathbf{s}_l^{k+1} = \mathbf{s}_l^k - \frac{1}{2}\mathbf{D}\mathbf{g}(\mathbf{s}_l^k) + \mathbf{D}^{\frac{1}{2}}\mathbf{w}_l \tag{9}$$

where the diagonal matrix $\mathbf{D}^{\frac{1}{2}}$ contains the discrete time steps $\tau_{l,n}$, $n = 1 : N$, so that, for the ith pixel, the diffusion coefficient is $\mathbf{D}_{n,n} = \tau^2_{l,n}$. Matrix $\mathbf{D}$ is referred to here as diffusion matrix. We determine it by taking the inverse of the diagonal of the Hessian matrix of $-\log p(\mathbf{s}_l|\mathbf{y}_{1:K}, \mathbf{s}_{(1:L)-l}, \mathbf{A}, \Theta)$. Rather than the expectation of the inverse of Hessian matrix, we use its diagonal calculated by the value of $\mathbf{s}_l$ at the discrete time k [4].

Since the random variables for the image pixel intensities are produced in parallel by using (9), the procedure is faster than the random walk process adopted in [14]. The derivation details of the equation can be found in [4]. After the sample production process, the samples are applied to a Metropolis-Hastings [15] scheme pixel-by-pixel.

4.3. Parameters of t-distribution

We find the mode estimates of the parameters of the t-distribution using EM method. We can write the posterior of the parameters such that $p(\alpha_{l,d}, \beta_{l,d}, \delta_{l,d}|\mathbf{t}_{l,d}, \Theta_{-\{\alpha_{l,d},\beta_{l,d},\delta_{l,d}\}}) = p(\mathbf{t}_{l,d}|\Theta)p(\beta_{l,d})$. In EM method, instead of maximizing the $\log\{p(\mathbf{t}_{l,d}|\Theta)p(\beta_{l,d})\}$, we maximize the following function iteratively

$$\Theta^{k+1} = \arg\max_{\Theta} Q(\Theta; \Theta^k) \tag{10}$$

where superscript k represents the iteration number and

$$Q(\Theta; \Theta^k) = \left\langle \log\{p(\mathbf{t}_{l,d}|\Theta)p(\beta_{l,d}))\}\right\rangle_{\nu_{l,d}|\mathbf{t}^k_{l,d},\Theta^k} \tag{11}$$

where $p(\nu_{l,d}|\mathbf{t}^k_{l,d}, \Theta^k)$ is the posterior density of the hidden variable $\nu_{l,d}$ conditioned on parameters estimated in the previous step k and $\langle . \rangle_{\nu_{l,d}|\mathbf{t}^k_{l,d},\Theta^k}$ represents the expectation with respect to $\nu_{l,d}|\mathbf{t}^k_{l,d}, \Theta^k$.

In the E (expectation) step of the EM algorithm, we must calculate the expectation $\langle . \rangle_{\nu_{l,d}|\mathbf{t}_{l,d}^k,\Theta^k}$. The posterior expectation of $\nu_{l,d}$ is found as [4]

$$\langle \nu_{l,d} \rangle = \frac{N + \beta_{l,d}^k}{\beta_{l,d}^k} \left(1 + \frac{\phi_d(\mathbf{s}_l^k, \alpha_{l,d}^k)}{\beta_{l,d}^k \delta_{l,d}^k} \right)^{-1} \tag{12}$$

In the M (maximization) step, (11) is maximized with respect to Θ. To maximize this function, we alternate among the variables $\alpha_{l,d}$, $\beta_{l,d}$ and $\delta_{l,d}$.

5. Simulation Results

We assume that the parametric mixing matrix is previously estimated with a known error. The parametric model is formed such that the column of synchrotron and dust varying according to power laws which depend on only one spectral index. To determine these spectral indices, we can use the FDCCA [18], [17] method. We have fixed the column of CMB because it is known. We obtain the realistic observations by mixing components with a mixing matrix which is formed by using the spectral indices 2.9 for synchrotron and 1.8 for dust. In this experiment, we assume that the spectral index of synchrotron dust have been estimated with an error 6.9% and 2% respectively. So, along the reconstruction algorithm, we fix the mixing matrix values such that the spectral indices equal to 2.7 for synchrotron and 1.78 for dust. We determine the blurring function according to antenna apertures. We model the aperture functions as Gaussian shape functions.

We have tested our algorithm on five different 128x128 pixel patches that are arranged on the vertical axis centered at galactic coordinates (00,00), (00,20), (00,40), (00,60) and (00,80). Fig. 1, shows the observations at (00,40). Fig. 2 shows the estimated map located at the coordinate of (0,40). We compare our proposed method with the LS and DB+LS solutions. In DB+LS, we first apply a de-blurring (DB) process to observation channels, then find the LS solution. We also compare the results of the proposed LS+ALS with those obtained by LS+ALS without considering the blurring of the psf. The PSIR values are placed at the top of each map. For the patch (0,40) in Fig. 2, the proposed method is better to reconstruct CMB and synchrotron maps in the sense of PSIR. The DB+LS method gives good results for dust map. The PSIR values of the patches (00,00), (00,20), (00,60) and (00,80) can be seen in Table 1. Fig. 3 compares the standard power spectrum of the ground-truth maps and those are obtained by LS, DB+LS and proposed LS+ALS without (without: w/o) psf and proposed LS+ALS with (with: w/) psf results.

6. Conclusion

The proposed method gives better reconstructions in both the pixel and the frequency domains, if compared with the intuitive basic methods. The algorithm works quite well at high galactic latitudes. If we approach the galactic plane, the estimation results get worse. Especially at the galactic plane, we have obtained the worst results, although we have used a different initialization strategy. We plan to extend this study by considering more sources and including error estimation results.

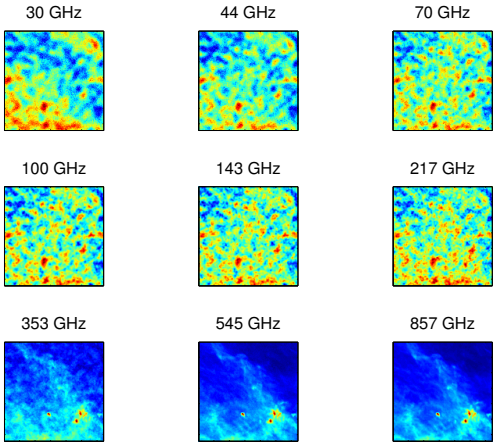

Figure 1: The blurred and noisy observations located at 0° longitude and 40° latitude. The map size is 128×128 pixels.

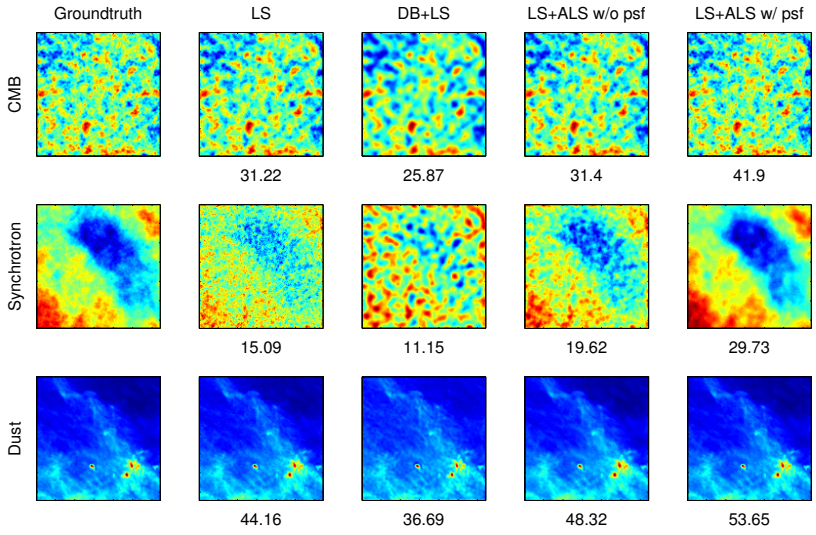

Figure 2: Estimated maps from blurred and noisy observations with the LS, DB+LS, LS+ALS without (w/o) psf and proposed LS+ALS with (w/) psf methods. The location of the patch is 0° longitude and 40° latitude. The PSIR values are placed under each map.

Table 1: The PSIR (dB) values of the separated components, in the pixel domain.

0,0

	CMB	Synchrotron	Dust
LS+ALS w/ psf	**21.82**	**42.85**	96.79
LS	17.41	36.88	77.86
DB+LS	19.26	39.29	**96.89**
LS+ALS w/o psf	18.09	39.59	77.36

0,20

	CMB	Synchrotron	Dust
LS+ALS w/ psf	**40.71**	**36.48**	**93.47**
LS	30.63	23.28	80.88
DB+LS	31.74	24.05	83.61
LS+ALS w/o psf	31.25	27.00	82.37

0,60

	CMB	Synchrotron	Dust
LS+ALS w/ psf	**41.42**	**33.48**	**35.50**
LS	30.62	18.24	24.12
DB+LS	33.95	17.99	24.85
LS+ALS w/o psf	30.76	22.65	29.76

0,80

	CMB	Synchrotron	Dust
LS+ALS w/ psf	**42.10**	**33.27**	**41.65**
LS	31.44	17.75	30.98
DB+LS	34.78	17.79	31.64
LS+ALS w/o psf	31.51	22.79	34.04

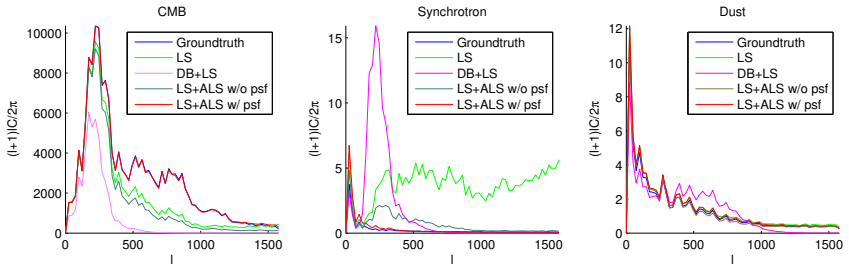

Figure 3: Comparison of the standard power spectrum of ground-truth maps (in Fig. 2) located at 0° longitude and 40° latitude with the LS, DB+LS, LS+ALS without (w/o) psf and proposed LS+ALS with (w/) psf results.

Acknowledgment

The authors would like to thank Anna Bonaldi,(INAF, Padova, Italy), Bulent Sankur, (Bogazici University, Turkey) and Luigi Bedini (ISTI, CNR, Italy) for valuable discussions. The simulated source maps are taken from the Planck Sky Model, a set of maps and tools for generating realistic Planck simulations made available thanks to the efforts of the Planck Working Group 2 (WG2) team. Some of the results in this paper have been derived using the HEALPix [19] package.

References

[1] D. Maino, A. Farusi, C. Baccigalupi, F. Perrotta, A. J. Banday, L. Bedini, C. Burigana, G. De Zotti, K. M. Górski, and E. Salerno, "All-sky astrophysical component separation with fast independent component analysis (FastICA)," Mon. Not. R. Astron. Soc., vol. 334, no. 1, (2002) pp. 53–68.

[2] J.-F. Cardoso, H. Snoussi, J. Delabrouille and G. Patanchon "Blind separation of noisy Gaussian stationary sources: Application to cosmic microwave background imaging, European. Conf. on Signal Processing, EUSIPCO'02, pp. 561–564, Toulouse, Sep. 2002.

[3] L. Bedini, D. Herranz, E. Salerno, C. Baccigalupi, E. E. Kuruoğlu and A. Tonazzini, "Separation of correlated astrophysical sources using multiple-lag data covariance matrices," EURASIP Journal on Applied Signal Processing, vol. 15 (2005) pp. 2400–2412.

[4] K. Kayabol, E. E. Kuruoglu, J. L. Sanz, B. Sankur, E. Salerno and D. Herranz, "Adaptive Langevin sampler for separation of *t*-distribution modelled astrophysical Maps," to be published IEEE Trans. Image Process., vol.19, no.9, (2010).

[5] M. Castella and J.-C. Pesquet, "An iterative blind source separation method for convolutive mixtures of images," ICA 2004, LNCS, vol. 3195 (2004) pp. 922–929.

[6] S. Anthoine, "Different Wavelet-Based Approaches for the Separation of Noisy and Blurred Mixtures of Components. Application to Astrophysical Data." PhD Thesis, Princeton University, 2005.

[7] A. Tonazzini and I. Gerace, "Bayesian MRF-based blind source separation of convolutive mixtures of images," in European Conf. Signal Process., EUSIPCO'05, Antalya, Turkey, Sep. 2005.

[8] S. Shwartz, Y. Y. Schechner and M. Zibulevsky, "Blind separation of convolutive image mixtures," Neurocomputing, vol. 71 (2008) 2164–2179.

[9] A. Tonazzini, I. Gerace and F. Martinelli "Multichannel blind separation and deconvolution of images for document analysis," IEEE Trans. Image Process., vol.19, no.4, (2010) pp. 912-925.

[10] D. Higdon, "Spatial Applications of Markov Chain Monte Carlo for Bayesian Inference." PhD Thesis, University of Washingthon, 1994.

[11] I. Prudyus, S. Voloshynovskiy and A. Synyavskyy, "Wavelet-based MAP image denoising using provably better class of stochastic i.i.d. images models," in Int. Conf. on Telecomm. in Modern Satell., Cable and Broadcas. TELSIKS'01, pp. 583–586, Sep. 2001.

[12] G. Chantas, N. Galatsanos, A. Likas and M. Saunders, "Variational Bayesian image restoration based on a product of t-distributions image priors," IEEE Trans. Image Process., vol.17, no.10, (2008) pp. 1795–1805.

[13] D. Tzikas, A. Likas and N. Galatsanos, "Variational Bayesian sparse kernel-based blind image deconvolution with Student's-t priors," IEEE Trans. Image Process., vol.18, no.4, (2009) pp. 753-764.

[14] K. Kayabol, E. E. Kuruoglu and B. Sankur, "Bayesian separation of images modelled with MRFs using MCMC," IEEE Trans. Image Process., vol.18, no.5, (2009) pp. 982–994.

[15] W. K. Hastings, "Monte Carlo sampling methods using Markov chains and their applications," Biometrika", vol. 57, no. 1, (1970) pp. 97–109.

[16] C. Liu and D. B. Rubin, “ML estimation of the t distribution using EM and its extensions, ECM and ECME,” Statistica Sinica”, vol. 5, (1995) pp. 19–39.

[17] L. Bedini, and E. Salerno, “Extracting astrophysical source from channel-dependent convolutional mixtures by correlated component analysis in the frequency domain,” in Lecture Notes in Artificial Intelligence, vol. 4694, (2007) pp. 9–16, Springer-Verlag.

[18] S. Ricciardi, A. Bonaldi, P. Natoli, G. Polenta, C. Baccigalupi, E. Salerno, K. Kayabol, L. Bedini, G. De Zotti, “Correlated component analysis for diffuse component separation with error estimation on simulated Planck polarization data,” Mon. Not. R. Astron. Soc., published online, June (2010).

[19] K. M. Górski, E. Hivon, A. J. Banday, B. D. Wandelt, F. K. Hansen, M. Reinecke, M. Bartelmann, ”HEALPix: A framework for high-resolution discretization and fast analysis of data distributed on the sphere”, The Astrophysical Journal, vol 622, no. 2, (2005) pp. 759-771.